Monthly Notices of the ROYAL ASTRONOMICAL SOCIETY LETTERS

Mon. Not. R. Astron. Soc. **408,** L56–L60 (2010) doi:10.1111/j.1745-3933.2010.00927.x

The discovery of a very cool, very nearby brown dwarf in the Galactic plane

P. W. Lucas,[1⋆] C. G. Tinney,[2] Ben Burningham,[1] S. K. Leggett,[3] David J. Pinfield,[1] Richard Smart,[4] Hugh R. A. Jones,[1] Federico Marocco,[4] Robert J. Barber,[5] Sergei N. Yurchenko,[6] Jonathan Tennyson,[5] Miki Ishii,[7] Motohide Tamura,[8] Avril C. Day-Jones,[9] Andrew Adamson,[3,10] France Allard[11] and Derek Homeier[12]

[1]*Centre for Astrophysics Research, University of Hertfordshire, College Lane, Hatfield AL10 9AB*
[2]*Department of Astrophysics, University of New South Wales, NSW 2052, Australia*
[3]*Gemini Observatory, Northern Operations Centre, 670 North Aohoku Place, Hilo, HI 96720, USA*
[4]*INAF/Osservatorio Astronomico di Torino, Strada Osservatorio 20, 10025 Pino Torinese, Italy*
[5]*Department of Physics and Astronomy, University College London, London WC1E 6BT*
[6]*Technische Universität Dresden, Institut für Physikalische Chemie und Elektrochemie, D-01062 Dresden, Germany*
[7]*Subaru Telescope, National Astronomical Observatory of Japan, 650 N. A'ohoku Place, Hilo, HI 96720, USA*
[8]*National Astronomical Observatory of Japan, 2-21-1 Osawa, Mitaka, Tokyo 181-8588, Japan*
[9]*Universidad de Chile, Camino el Observatorio, #1515, Las Condes, Santiago, Chile, Casilla 36-D, Chile*
[10]*Joint Astronomy Centre, 660 N. A'ohoku Place, University Park, Hilo, HI 96720, USA*
[11]*CRAL, Universite de Lyon, École Normale Supérieur, 46 allee d'Italie, 69364 Lyon Cedex 07, France*
[12]*Institut für Astrophysik Göttingen, Georg-August-Universität, Friedrich-Hund-Platz 1, D-37077 Göttingen, Germany*

Accepted 2010 July 28. Received 2010 July 28; in original form 2010 June 22

ABSTRACT

We report the discovery of a very cool, isolated brown dwarf, UGPS 0722−05, with the United Kingdom Infrared Telescope Deep Sky Survey (UKIDSS) Galactic Plane Survey. The near-infrared spectrum displays deeper H_2O and CH_4 troughs than the coolest known T dwarfs and an unidentified absorption feature at 1.275 μm. We provisionally classify the object as a T10 dwarf but note that it may in future come to be regarded as the first example of a new spectral type. The distance is measured by trigonometric parallax as $d = 4.1^{+0.6}_{-0.5}$ pc, making it the closest known isolated brown dwarf. With the aid of *Spitzer*/Infrared Array Camera (IRAC) we measure $H - [4.5] = 4.71$. It is the coolest brown dwarf presently known – the only known T dwarf that is redder in $H - [4.5]$ is the peculiar T7.5 dwarf SDSS J1416+13B, which is thought to be warmer and more luminous than UGPS 0722−05. Our measurement of the luminosity, aided by Gemini/T-ReCS N-band photometry, is $L = 9.2 \pm 3.1 \times 10^{-7}\,L_{\odot}$. Using a comparison with well-studied T8.5 and T9 dwarfs we deduce $T_{\rm eff} = 520 \pm 40$ K. This is supported by predictions of the Saumon & Marley models. With apparent magnitude $J = 16.52$, UGPS 0722−05 is the brightest of the ∼90 T dwarfs discovered by UKIDSS so far. It offers opportunities for future study via high-resolution near-infrared spectroscopy and spectroscopy in the thermal infrared.

Key words: surveys – brown dwarfs – stars: low mass.

1 INTRODUCTION

In the past 15 yr ∼200 T dwarfs have been discovered in the local field with the Two Micron All Sky Survey (2MASS), the Sloan Digital Sky Survey (SDSS) and the United Kingdom Infrared Telescope Deep Sky Survey (UKIDSS) (see e.g. Leggett et al. 2000; Burgasser et al. 2002; Burningham et al. 2010a). These discoveries are useful for investigating the substellar mass function. Searches in young clusters, e.g. Lodieu et al. (2007), Weights et al. (2009) and Luhman (2004) suggest that the ratio of brown dwarfs to stars is between ∼1:6 and ∼1:3 (excluding companions), but there are growing indications that fewer exist in the local field (e.g. Burningham et al. 2010a). The nearest isolated brown dwarfs known until now (LP944−20, DENIS-P J025503.5−470050, DENIS J081730.0−615520) are located at distances $d = 4.9$–5.0 pc

⋆E-mail: p.w.lucas@herts.ac.uk

from the Sun (Tinney 1998; Costa et al. 2006; Artigau et al. 2010). These are the 46th, 48th and 49th nearest systems. If the mass function in the local field is similar to that in young clusters, then we should expect that some brown dwarf primaries remain undiscovered at $d < 5$ pc. Most such objects would have to have types $\geq$T8.5 in order to lie below the 2MASS detection limit (Skrutskie et al. 2006).

The UKIDSS Large Area Survey (LAS; Lawrence et al. 2007) has discovered several brown dwarfs cooler than those found by 2MASS (e.g. Warren et al. 2007; Burningham et al. 2008, hereafter B08; Burningham et al. 2010b). The Canada–France–Hawaii Telescope (CFHT) Brown Dwarf Survey has yielded two similar discoveries (e.g. Delorme et al. 2008). Most of these objects have been classified as T8.5 or T9 dwarfs because the broad H_2O and CH_4 absorption bands in their near-infrared spectra are slightly deeper than those of T8 dwarfs. The slight differences in the spectra belie a large drop in effective temperature from 700–800 K at T8 to 500–600 K for the coolest objects (B08; Leggett et al. 2010a, hereafter L10a). Here we report the discovery in the UKIDSS Galactic Plane Survey (GPS; Lucas et al. 2008, hereafter L08) of UGPS J072227.51−054031.2 (hereafter UGPS 0722−05), an even cooler and less luminous brown dwarf. The GPS is not optimal for late T dwarf searches since it employs only the J, H and K filters. For objects with negative $H - K$ colours, the GPS probes less than a quarter of the volume of the LAS for the same area of sky. Source confusion is also a serious impediment in much of the GPS area.

2 CANDIDATE SELECTION

UGPS 0722−05 was identified as the only good candidate late-T or Y dwarf amongst the 604 million sources in GPS sixth Data Release to satisfy the colour criteria $J - H < -0.2$ mag, $H - K < -0.1$ mag. We used several data quality restrictions to minimize the number of false candidates (see L08). The criteria were jmhPntErr < 0.3, hmk_1PntErr < 0.3 (limiting the uncertainty in source colours); jppErrbits < 256, hppErrbits < 256, k_1ppErrbits < 256 (removes sources with photometric quality warnings); pstar > 0.9 (requires a point-source image profile); jEll < 0.3, hEll < 0.3, k_1Ell < 0.3 (limits on ellipticity); $\sqrt{}$(hXi^2+hEta^2) < 0.3, $\sqrt{}$(k_1Xi^2+k_1Eta^2) < 0.3 (limits on coordinate shifts between passbands).

A further constraint was to limit the search to Galactic longitudes $l > 60^\circ$ and $l < 358^\circ$. These restrictions were designed to select against blended stellar pairs with inaccurate photometry, which are a frequent occurrence in the most crowded regions of the plane. Only six candidates remained after this procedure. Of these, four were revealed as blended stellar pairs or defective data by inspection of the images and one (a candidate white dwarf) was ruled out by its detection in visible light in the POSS USNO-B1.0 archive. An image of the remaining candidate, UGPS 0722−05, is shown in Fig. 1. The coordinates measured on 2010 March 2 (see Section 3) were RA = $07^{\rm h}22^{\rm m}27\overset{\rm s}{.}29$, Dec. = $-05^{\rm d}40^{\rm m}30\overset{\rm s}{.}0$.

3 OBSERVATIONS

The Near-Infrared Imager and Spectrometer (NIRI) on the Gemini-North Telescope on Mauna Kea was used on 2010 February 10, 11 and 14 to take spectra covering the J, K and H bandpasses, respectively, with total on-source integration times of 16, 30 and 60 min, respectively. The spectral resolution was $R \sim 500$. They were reduced and calibrated with the IRAF software package using standard techniques (see e.g. Burningham et al. 2010a). The three spectra were then flux calibrated using the UKIDSS photometry and combined into a single spectrum.

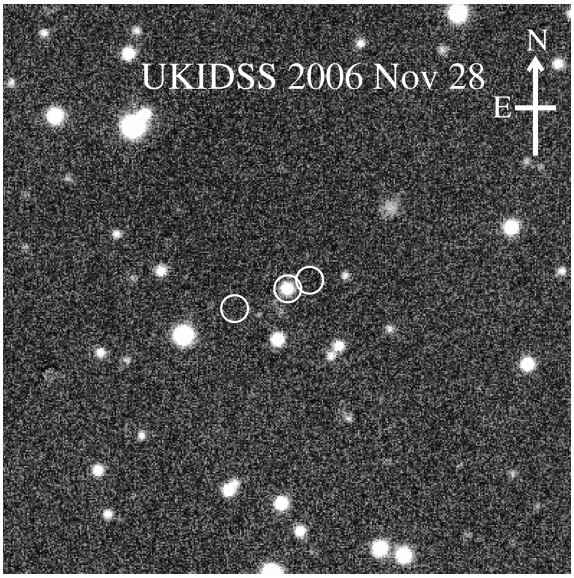

Figure 1. UKIDSS J-band discovery image (80 arcsec square). The circles illustrate the proper motion (see Table 3). The centre circle marks the position at the time of the discovery image in 2006, while the circles to the left- and right-hand side mark the positions at the time of the 2MASS image in 1998 and a UKIRT image from 2010 March 2, respectively.

The UKIDSS discovery images were taken on 2006 November 28. The NIRI acquisition images obtained 3.2 yr later showed that UGPS 0722−05 has a proper motion of $\sim$1 arcsec yr^{-1}. This then allowed the identification of UGPS 0722−05 with a previously uncatalogued source in the 2MASS Atlas image acquired with the 2MASS South telescope on 1998 October 19. A programme of parallax observations was then begun with the UKIRT Wide Field Camera, using the methods described in Smart et al. (2010). The object was observed in the J passband on 2010 February 19, March 2, 16, 30, April 13 and 27. All the UKIRT images had full width at half-maxima between 0.8 and 1.1 arcsec and used microstepping to yield a pixel scale of 0.20 arcsec. The total integration time on each occasion was 400 s.

The results of multiwaveband photometry are given in Table 1. All dates refer to 2010 except for the UKIDSS *JHK* photometry from 2006. The instruments listed are the Gemini Multi-Object Spectrograph (GMOS) on the Gemini-North Telescope; the Wide Field Camera (WFC) on the United Kingdom Infrared Telescope (UKIRT); the Infrared Array Camera (IRAC) on the *Spitzer Space Telescope*; the Infrared Camera and Spectrograph (IRCS) on the Subaru Telescope and the Thermal Region Camera Spectrograph (T-ReCS) on the Gemini-South Telescope.

All fluxes except i and z are Vega magnitudes. Data taken in the GMOS i and z filters and the WFC Z filter were transformed to the SDSS AB system using the far-red spectra of 16 dwarfs ranging in type from L3 to T8. The large uncertainty in the IRCS L' flux is due to uncertainty in the aperture correction, which arose from imperfect telescope tracking. The T-ReCS data were taken over two nights. Observing conditions were somewhat variable and the signal-to-noise ratio on each night was low. The final co-added image had a signal-to-noise ratio of 7. The photometric uncertainty given in Table 1 includes the uncertainties in the calibration and in the final aperture correction.

Table 1. Photometry of UGPS 0722−05.

	i	*z*	*z*	*Y*	*J*	*H*	*K*	[3.6]	[4.5]	*L*′	*N*	*J* − *H*	*H* − *K*
Magnitude	24.80	20.60	20.42	17.37	16.52	16.90	17.07	14.28	12.19	13.4	10.28	−0.38	−0.18
Error	0.13	0.07	0.06	0.02	0.02	0.02	0.08	0.05	0.04	0.3	0.24	0.03	0.08
Instrument	GMOS	GMOS	WFC	WFC	WFC	WFC	WFC	IRAC	IRAC	IRCS	T-ReCS		
Date	15/3	15/3	16/3	16/3	27/11	27/11	27/11	30/4	30/4	6/4	24/3; 13/4		
Exposure (s)	4800	120	400	120	80	80	40	1440	1440	335	3360		

4 RESULTS

4.1 Spectroscopy

The near-infrared spectrum of UGPS 0722−05 (Fig. 2, upper panel) is broadly similar to that of a T9 dwarf. However, a ratio plot comparing UGPS 0722−05 with the average of three T9 dwarfs (Fig. 2, middle panel) shows that the broad molecular absorption troughs on either side of the flux peaks at 1.28 and 1.59 μm and on the long-wavelength side of the 1.07 μm peak are between 10 and 30 per cent deeper. The values of the spectral indices 'W_J', 'CH_4-J', 'NH_3-H' and 'CH_4-H', which are used for typing the coolest T dwarfs (see B08) are smaller than those of T9 dwarfs by amounts similar to the differences between T8 and T9 dwarfs (see Table 2). We therefore assign a spectral type of T10. The expanded view of the *J*-band spectrum (Fig. 2, lower panel) shows a narrow absorption feature at 1.275 μm that has an equivalent width of 3.6 ± 0.1 Å. A feature has been seen at a similar wavelength in Jupiter and (weakly) in a T8.5 dwarf and a T9 dwarf (see B08). We have examined a synthetic NH_3 spectrum generated from a new high-temperature line list (see Yurchenko et al. 2009; Yurchenko et al., in preparation), but there is no sign of a corresponding feature. The only candidate NH_3 absorption feature in the spectrum is a weak detection in the *H* band, at 1.514 μm (not shown). This is the wavelength of the strongest feature produced by a group of lines at $1.4 < \lambda < 1.6\,\mu$m in the synthetic spectrum, when binned to the same resolution as the data. We caution that no conclusion can be drawn from this comparison until the line list is incorporated into a full model atmosphere.

In Fig. 2 (bottom panel) we overplot a BT-SETTL-model atmosphere spectrum (see Allard et al. 2007), computed for effective temperature $T_{\rm eff} = 500\,$K, $g = 10^4$ cm s^{-2} and [M/H] = 0.0. Comparison with the data indicates that some marginally detected narrow absorption features, e.g. at 1.282 μm, are probably real. Most of the narrow absorption features that appear in the model are due to H_2O (the NH_3 and CH_4 lists employed are highly incomplete in the *J* band). H_2O is a possible carrier of the 1.275-μm feature. Another is HF, which has some absorption lines at wavelengths close to this that are included in the models. This possibility was also suggested by Y. Pavlenko (private communication). Despite the reasonable qualitative agreement between the model and the data in the *J* band, the overall 1–2.5 μm spectral energy distributions (SEDs) predicted by all the BT-SETTL models at $T_{\rm eff} = 400$–600 K (not shown) are much bluer than we observe.

4.2 Parallax and proper motion

An astrometric analysis was performed using the UKIRT and 2MASS data with a sample of eight reference stars near UGPS 0722−05, using methods described in Tinney et al. (2003). The chosen stars surround the target, range in brightness from 1.9 mag brighter to 0.1 mag fainter than it (most are within 0.3 mag) and are found in both the 2MASS and UKIRT images. The scatter of the residuals about the astrometric solution for reference stars within ±0.2 mag of UGPS 0722−05 in UKIRT data is 6.2 mas. We adopt this as the astrometric precision for the T dwarf at each epoch.

The astrometric solution for UGPS 0722−05 using the UKIRT data alone clearly shows that it is nearby (see Table 3 – the relative parallax is the weighted mean of those arising from the right ascension and declination solutions). However, the non-optimal sampling of its proper motion results in some concerns about degeneracy impacting on the parallax solution. Fortunately, the 2MASS data help us to refine the solution. Even though the observation has low signal-to-noise ratio (the astrometric precision for the reference stars is ∼40 times lower than the UKIRT images), it adds in a much longer time baseline to constrain the proper motion. The UKIRT+2MASS solution (shown in Fig. 3 for the 2006–10 period) is consistent with the UKIRT-only solution (see Table 3), giving us confidence that the distance to this object has been well constrained. At $d = 4.1^{+0.6}_{-0.5}$ pc, UGPS 0722−05 is the closest isolated brown dwarf known. Two even closer stars with brown dwarf companions are known: ϵ Indi (Scholz et al. 2003) and SCR 1845−6357 (Biller et al. 2006). We note that neither the Gemini acquisition images (with 0.4-arcsec resolution) nor the *Spitzer* images reveal any sign of a companion. A proper motion search for companions with the SuperCosmos archive also found nothing.

5 ANALYSIS AND DISCUSSION

UGPS 0722−05 has absolute *J*-band magnitude, $M_J = 18.5 \pm 0.2$, which is fainter than any other brown dwarf. Marocco et al. (2010) have measured parallaxes for a large sample of T dwarfs and plotted M_J versus spectral type. Our assigned spectral type of T10 is consistent with the general trend that they report, within the scatter.

UGPS 0722−05 has $H - [4.5] = 4.71$, which is redder than any other brown dwarf except the metal-poor T7.5p dwarf SDSS J1416+13B (Burningham et al. 2010b). The $H - [4.5]$ colour is considered a good indicator of $T_{\rm eff}$ (see e.g. L10a), so this supports our inference from the near-infrared spectrum that UGPS 0722−05 is cooler than the three known T9 dwarfs, for which $4.0 \leq H - [4.5] \leq 4.5$. The $i - z, z - Y, Y - J, J - H$ and $H - K$ colours of the object are similar to those of the T9 dwarfs. While the $H - [4.5]$ colour is considered a good indicator of $T_{\rm eff}$, it is also influenced by metallicity and gravity (L10a). Recent estimates of the distance to SDSS 1416+13B ($d \approx 8$ pc; see Burgasser et al. 2010; Scholz 2010) indicate that it is more luminous than UGPS 0722−05 by a factor of ∼2. Assuming that these estimates are not greatly in error, they indicate that the redder colour of SDSS 1416+13B is due to a combination of low metallicity and high gravity, which would also explain the extremely blue $H - K$ colour (see e.g. Leggett et al. 2009). As Burgasser et al. (2010) pointed out, this implies

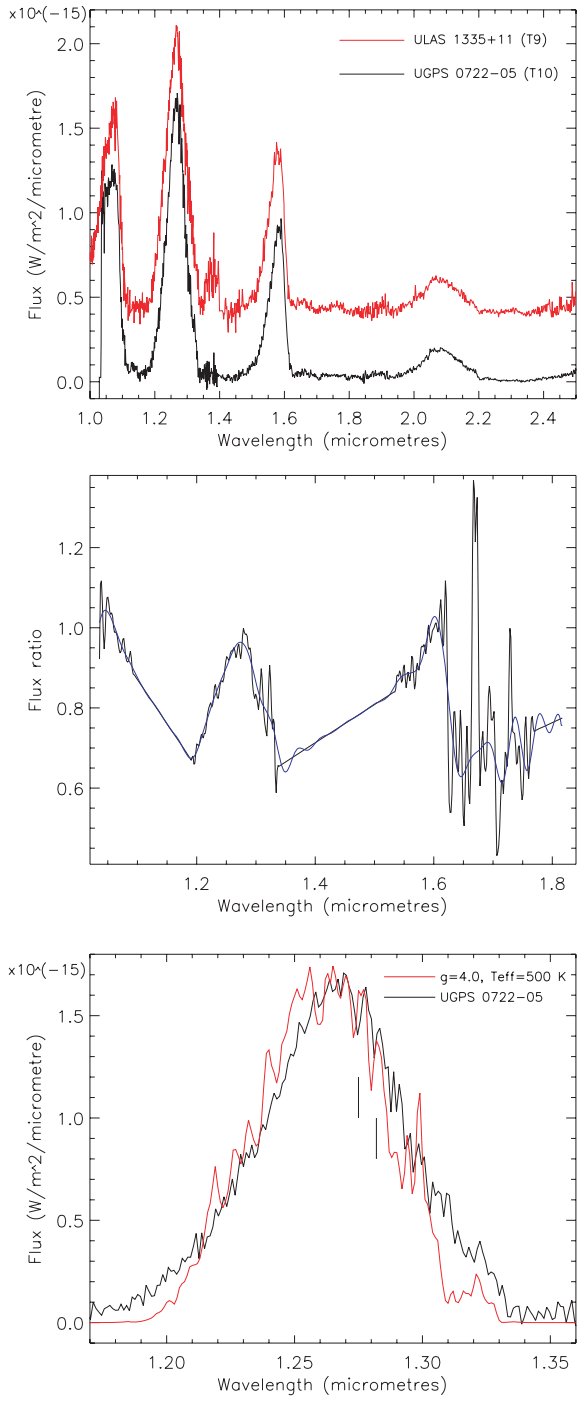

Figure 2. Upper panel: near-infrared spectrum of UGPS 0722−05 (black line) and a T9 dwarf shown suitably scaled and offset for comparison. Middle panel: a lightly smoothed ratio spectrum (black line) showing the 1.05–1.8 μm region of the UGPS 0722−05 spectrum divided by the average of three T9 dwarf spectra and normalized to unity at 1.279 μm. The blue curve shows a high-order polynomial fit to the black line (the noise feature at 1.67 μm was excluded from the fit). This plot shows clearly that the broad molecular absorption bands in UGPS 0722−05 are deeper on either side of the flux peaks near 1.27 and 1.59 μm, and on the long-wavelength side of the 1.07-μm peak. Straight lines interpolate across noisy regions where there is little flux. Lower panel: expanded view of the *J*-band spectrum with a BT-SETTL model overplotted, normalized to the same flux at 1.27 μm. Vertical lines mark the absorption features at 1.275 and 1.282 μm.

that the $T_{\rm eff}$ of SDSS 1416+13B is somewhat higher than the 500-K value that Burningham et al. (2010b) derived from the colours in the absence of a significant luminosity constraint. We therefore conclude that UGPS 0722−05 is the coolest brown dwarf known.

To calculate the total luminosity of the object we summed over the SED as follows. The flux-calibrated near-infrared spectrum covers the range $1.035 < \lambda < 2.54$ μm. For 0.94–1.035 μm we used the spectrum of the T9 dwarf ULAS J003402.77−005206.7 (hereafter 0034−00; Warren et al. 2007), scaled to the *Y* magnitude of UGPS 0722−05. The negligible flux at $\lambda < 0.94$ μm was not included. For 3.92–4.00 μm we used the spectrum of the T8 dwarf 2MASS J04151954−0935066 (hereafter 0415−09; Saumon et al. 2007, hereafter S07), scaling to the 3.6-μm flux. The fluxes in the 3.6-μm IRAC and T-ReCS *N* (7.7–13.0 μm) passbands were calculated using the flux-calibrated spectra of 0415−09 (S07) and the T9 dwarf ULAS J133553.45+113005.2 (hereafter 1335+11; Leggett et al. 2009), respectively. BT-SETTL models with $T_{\rm eff}$ = 500–600 K and log(*g*) = 4.0–5.0, [M/H] = 0.0 were used for the 4.5-μm magnitude to flux conversion (lacking a suitable measured spectrum). The same models were used to estimate the flux at $\lambda > 13.0$ μm, at 2.54–3.18 μm and at 5.02–7.70 μm, scaling with the aid of fluxes in adjacent measured passbands. The fluxes in these wavelength intervals have large uncertainties, owing to a strong dependence on model parameters.

The total luminosity of UGPS 0722−05 is $L = 9.2 \pm 3.1 \times 10^{-7}$ L$_\odot$, where the uncertainty arises from a 19 per cent uncertainty in the total flux and the 13 per cent uncertainty in the distance. This compares with $L = 1.1 \pm 0.1 \times 10^{-6}$ L$_\odot$ for the T9 dwarfs 0034−00 and 1335+11 (Marocco et al. 2010) and $L = 9.8 \pm 0.1 \times 10^{-7}$ L$_\odot$ for the T8.5 dwarf Wolf 940B (Leggett et al. 2010b), all of which have more fully measured SEDs and much more precise parallaxes.

Assuming an age in the range of 0.2–10 Gyr, the evolutionary models of Saumon & Marley (2008, hereafter SM08), allow a radius, *R*, between 0.085 R$_\odot$ (at 10 Gyr) and 0.12 R$_\odot$ (at 0.2 Gyr). Using the definition of $T_{\rm eff}$, $L = 4\pi R^2 \sigma T_{\rm eff}^4$, we calculate $T_{\rm eff} = 614 \pm 46$ K for $R = 0.085$ R$_\odot$ and $T_{\rm eff} = 516 \pm 39$ K for $R = 0.12$ R$_\odot$.

Model atmospheres are not presently considered to be reliable at such low temperatures. None the less, some indication of physical properties can be gained by consideration of evolutionary models and model atmospheres, aided by comparison with other late T dwarfs (see e.g. L10a). UGPS 0722−05 has $H - K = -0.18 \pm 0.08$ and $M_H \approx 18.8$. In the top panel of fig. 9 of L10a it would lie at the bottom of the plot under Wolf 940B, indicating that the dwarf has similar gravity and metallicity to the T9 dwarfs 0034−00 and 1335+11 but is significantly cooler, with $T_{\rm eff} \approx 500$ K. Exactly the same conclusion can be drawn from placing it in the $H - K$ versus $H - [4.5]$ diagram in fig. 7 of Leggett et al. (2009). The similarity otherwise to the three T8.5 to T9 dwarfs implies that UGPS 0722−05 has solar or slightly enhanced over solar metallicity. Its small tangential velocity (∼19 km s^{-1}) suggests that it is not a very old object.

The luminosity calculation permits effective temperatures in the range of 477–660 K (allowing for the uncertainties in *L* and *R*). However, similar calculations for the T9 dwarfs 0034−00 and 1335+11 (which have well-measured luminosities), find $T_{\rm eff}$ = 530–660 K for both objects (Marocco et al. 2010) and models indicate $T_{\rm eff} <$ 600 K for 1335+11 (B08; Leggett et al. 2009; L10a). The mature age-benchmark T8.5 dwarf Wolf940 B has $T_{\rm eff} \approx 600$ K (Leggett et al. 2010b), which is based on a well-measured luminosity and a well-constrained radius. Since UGPS 0722−05 is clearly cooler than these three objects, which have bluer $H - [4.5]$ colours and earlier spectral types, we can be confident that its effective temperature

Table 2. Spectral indices for very cool brown dwarfs. Numbers in brackets are the uncertainties on the last two digits.

Object	W_J	H_2O-J	CH_4-J	NH_3-H	H_2O-H	CH_4-H	CH_4-K	K/J
UGPS 0722−05	0.2074(12)	0.0339(17)	0.1358(19)	0.4917(21)	0.1218(17)	0.0643(13)	0.0959(22)	0.12615(33)
T9 average	0.258	0.025	0.162	0.535	0.122	0.086	0.104	0.121
T8 0415−09	0.31	0.030	0.168	0.625	0.173	0.105	0.05	0.134

Table 3. Astrometric solution for UGPS 0722−05.

Solution	No. of epochs	μ (mas yr^{-1})	θ (°)	π (mas)
UKIRT only	7	972 ± 8	291.2 ± 0.2	237 ± 41
UKIRT+2MASS	8	967 ± 8	291.1 ± 0.2	246 ± 33

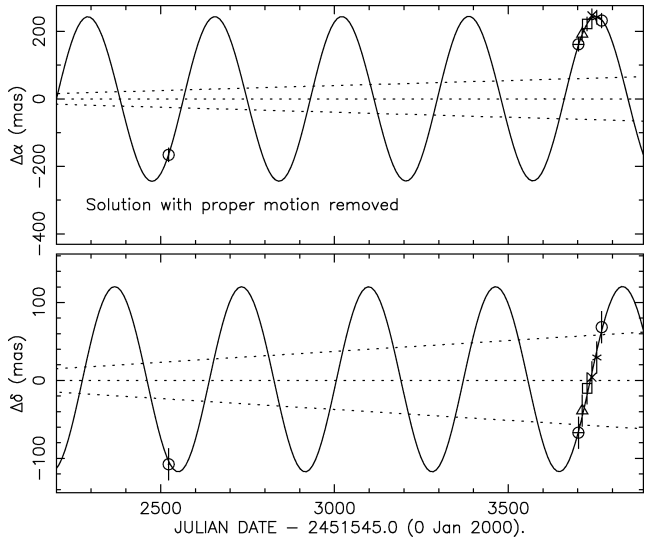

Figure 3. The UKIRT+2MASS astrometric fit, shown for 2006–2010 after proper motion (PM) subtraction. Dotted lines show the PM uncertainties.

is in the lower half of the range permitted by the luminosity. We adopt $T_{\rm eff} = 480$–560 K as the most likely range for this object. This is consistent with the 500-K value indicated by the SM08 models. At 480–560 K, the SM08 models indicate a mass in the range of 5–15 $M_{\rm Jup}$, $\log(g) = 4.0$–4.5 and age of 0.2–2.0 Gyr.

Whilst we have provisionally designated it as a T10 dwarf, we note that it is usual for the range of subtypes to run from 0 to 9. It is therefore quite possible that UGPS 0722−05 will come to be seen as the first example of a new spectral type. The fairly strong 1.275-μm feature might perhaps form the basis of such a classification. Gross changes in the 1–2.5 μm spectra are not expected in cooler objects, given the similarity of T dwarf spectra to that of Jupiter (see B08), but the near-infrared component of the SED will decline.

ACKNOWLEDGMENTS

The identification of the single good candidate late T dwarf found amongst several hundred million stars in the UKIDSS GPS is a tribute to the quality of UKIRT and the expertise of the staff at the Joint Astronomy Centre, the Cambridge Astronomical Survey Unit and the Wide Field Astronomy Unit at Edinburgh University. UKIRT is operated by the Joint Astronomy Centre on behalf of the Science and Technology Facilities Council of the UK. Gemini is operated by the Association of Universities for Research in Astronomy, Inc., under a cooperative agreement with the NSF on behalf of the Gemini partnership, which consists of national scientific organizations in the USA, the UK, Canada, Chile, Australia, Brazil and Argentina (see www.gemini.edu). The Subaru Telescope is operated by the National Astronomical Observatory of Japan. This research has made use of the USNOFS Image and Catalogue Archive operated by the United States Naval Observatory, Flagstaff Station. CGT acknowledges the support of ARC grant DP0774000.

REFERENCES

Allard F. et al., 2007, A&A, 474, L21
Artigau E. et al., 2010, ApJ, 718, L38
Biller B. A. et al., 2006, ApJ, 641, L141
Burgasser A. J. et al., 2002, ApJ, 564, 421
Burgasser A. J., Looper D., Rayner J. T., 2010, AJ, 139, 2448
Burningham B. et al., 2008, MNRAS, 391, 320 (B08)
Burningham B. et al., 2010a, MNRAS, 406, 1885
Burningham B. et al., 2010b, MNRAS, 404, 1952
Costa E. et al., 2006, AJ, 132, 1234
Delorme P. et al., 2008, A&A, 482, 961
Lawrence A. et al., 2007, MNRAS, 379, 1599
Leggett S. K. et al., 2000, ApJ, 536, L35
Leggett S. K. et al., 2009, ApJ, 695, 1517
Leggett S. K. et al., 2010a, ApJ, 710, 1627 (L10a)
Leggett S. K. et al., 2010b, ApJ, 720, 252
Lodieu N. et al., 2007, MNRAS, 380, 712
Lucas P. W. et al., 2008, MNRAS, 391, 136 (L08)
Luhman K. L., 2004, ApJ, 617, 1216
Marocco F. et al., 2010, A&A, submitted
Saumon D., Marley M. S., 2008, ApJ, 689, 1327 (SM08)
Saumon D. et al., 2007, ApJ, 656, 1136 (S07)
Scholz R.-D., 2010, A&A, 510, L8
Scholz R.-D. et al., 2003, A&A, 398, L29
Skrutskie M. F. et al., 2006, AJ, 131, 1163
Smart R. et al., 2010, A&A, 511, A30
Tinney C. G., 1998, MNRAS, 296, L42
Tinney C. G., Burgasser A. J., Kirkpatrick J. D., 2003, AJ, 126, 975
Warren S. J. et al., 2007, MNRAS, 381, 1400
Weights D. J. et al., 2009, MNRAS, 399, 2288
Yurchenko S. N. et al., 2009, J. Phys. Chem. A., 113, 11845

This paper has been typeset from a TEX/LATEX file prepared by the author.